FSW Development in aerospace industries

By: AHMED SAMIR

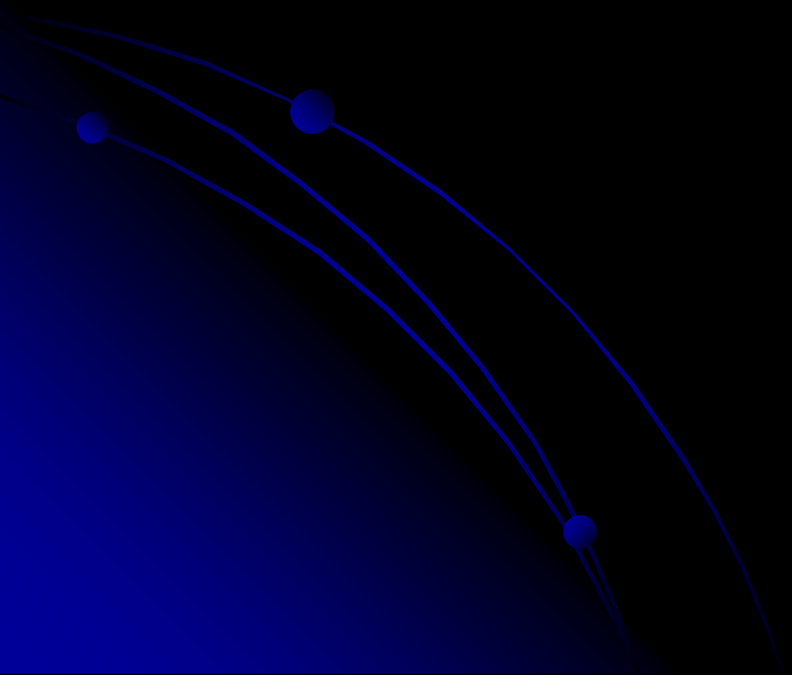

OVERVIEW

1. Introduction
2. Experimental Method/Setup
3. Mechanical Models
4. Simulation
5. Results
6. Conclusions
7. Current and Future Work

INTRODUCTION

- Current uses of FSW:
  - Aerospace (Spirit, Boeing, Airbus)
  - Railway (Hitachi Rail)
  - Shipbuilding/marine (Naval vessels)
  - Construction industries and others (Audi)
- Moving to lighter materials (e.g. Aluminum)
- Conflict: 3-D contours difficult with heavy duty machine tool type equipment

INTRODUCTION

- Ideally see widely applicable industrial robots equipped for FSW
- Benefits:
  - lower costs
  - energy efficient
  - 3-D contours etc.
- Problem: High axial forces required to FSW (1-12+ kN or 225-2700+ lbs), difficult to maintain even using robust robots especially at large distances from the base unit
- Possible solution: Utilize increased rotational speed/decreased axial force relationship to aid in developing a larger operational envelope for high speed FSW

EXPERIMENTAL METHOD

- Purpose: Examine axial forces during high speed friction stir welding with respect to mechanistic defect development due to process parameter variation

- Two Mechanical Models
  - Smooth Tool Pin (Preliminary)
  - Threaded Tool Pin (More Comprehensive)

- Parameters (Variables)
  - Rotational Speed (RS)
  - Travel Speed (TS)

EXPERIMENTAL METHOD

- Model solved with CFD package FLUENT for steady state solutions
- Force simulated for the three spatial dimensions as well as torque
- Experimental force and torque data recorded using a Kistler dynamometer (RCD) Type 9124 B

EXPERIMENTAL SETUP

- VU FSW Test Bed: Milwaukee #2K Universal Milling Machine utilizing a Kearney and Treker Heavy Duty Vertical Head Attachment modified to accommodate high spindle speeds.

- Samples- AA 6061-T6: 76.2 x 457.2 x 6.35 mm (3 x 18 x ¼")

- Rotational Speeds: 1000-5000 RPM

- Travel Speeds: 290 - 1600 mm min^{-1} (11.4 in min^{-1} – 63 in min^{-1})

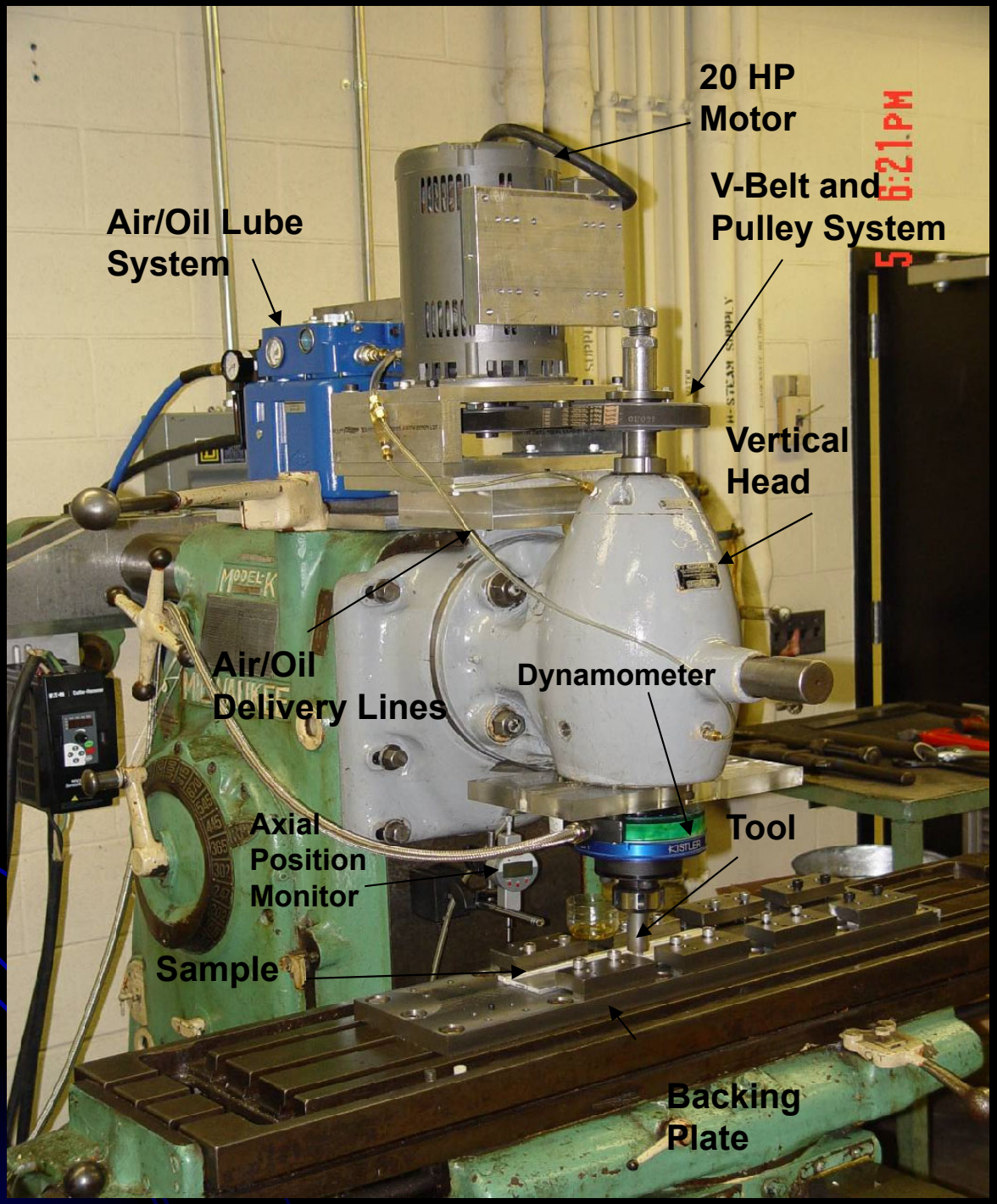

VANDERBILT WELDING AUTOMATION LABORATORY

VUWAL Test Bed

EXPERIMENTAL SETUP

- The tool was set up for a constant 2^{o} lead angle
- Fine adjustments in plunge depth have been noted to create significant changes in force data as well as excess flash buildup
- Therefore, significant care and effort was put forth to ensure constant plunge depth of 3.683 mm (.145”)
- Shoulder plunge constant: .1016 mm (.0040 in)

SMOOTH PIN MODEL

- Heat transfer to the support anvil ignored
- Tool pin and sample finite element mesh consists of
  - 22497 tetrahedron brick elements
  - 5152 nodes
- Tool properties were for H-13 tool steel (e.g. density, specific heat, and thermal conductivity)
- Assumed to rotate counter-clockwise at RS (LH)
- 12.7 mm shank included to account for heat conduction from the tool/sample interface

SMOOTH PIN MODEL

- Tool assumed to rotate with uniform and constant angular velocity, RS.
- Weld material is assumed incoming from the left upon the rotating tool
- Origin of the system is interface at the center of the pin bottom and the sample
- Sample given metallurgic properties (i.e. AA6061-T6)

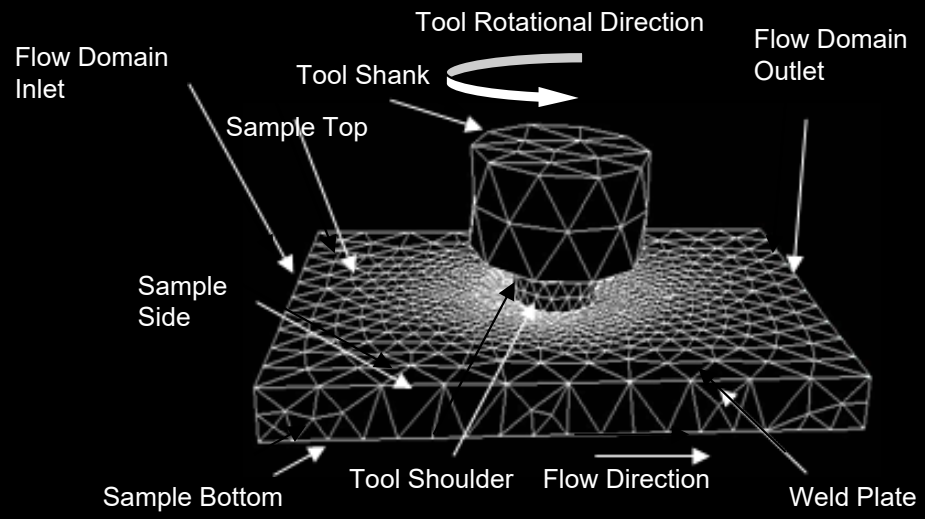

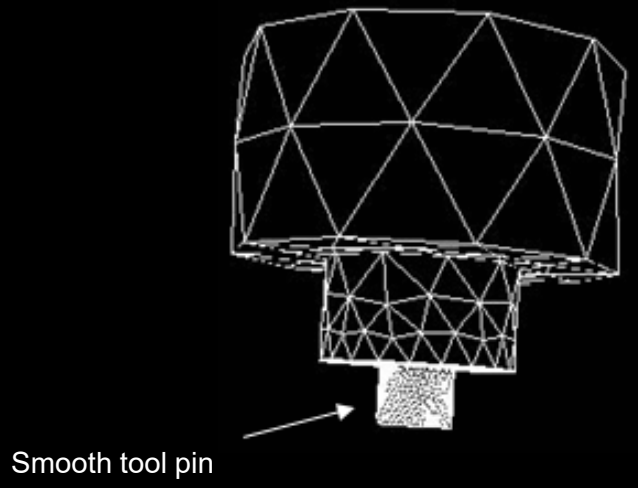

THREADED PIN MODEL

- 2nd Model incorporates the #10-24 TPI Left-Handed thread
- Incorporates the threaded tool pin, and heat sinks on the shank
- Heat conductivity to the anvil is included
- Identical metallurgic properties given to pin and sample as the smooth pin model
- Anvil properties - Cold rolled steel

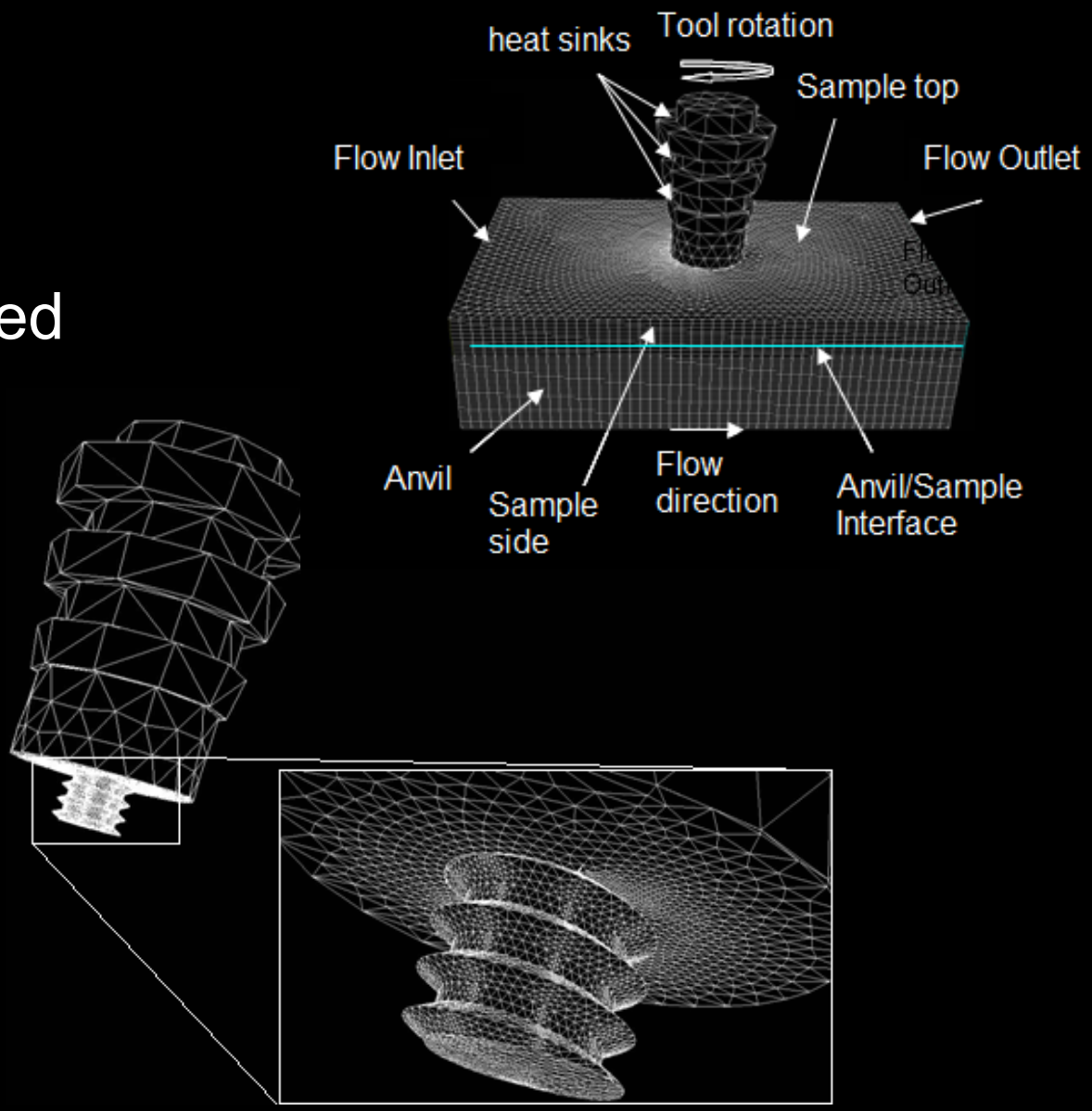

THREADED PIN MODEL

- Tool mesh:
  - 37051 tetrahedron brick elements
  - 8324 nodes
- Sample mesh:
  - 92018 tetrahedron brick elements
  - 20672 nodes
- Anvil mesh:
  - 42200 quadrilateral brick elements
  - 24024 nodes
- Density of mesh increases with respect to the pin/weld material interface

FLUENT: ASSIGNMENTS AND ASSUMPTIONS

- Goal: Compare the two models' steady state welding conditions with experimentally determined data
- Flow inlet given constant flow rate (TS)
- Zero heat flux condition
  - bounding regions transfer no heat to/from the weld
- No-slip (sticking) condition
  - all rotational velocity of the tool is transmitted to the weld material at the interface
- Temperature was simulated for both mechanical models

TEMPERATURE SIMULATION

- Temperature was simulated using the heat generation model developed by Schmidt H. et al. The contact stress is approximated as,

$$\tau_{contact} = \frac{\sigma_{yield}}{\sqrt{3}}$$

σ_{yield} = 241 MPa, AA 6061-T6

•The total heat generation approximated as:

$$Q_T = \frac{2}{3}\pi\tau_{contact}\,\omega_o\left(R_s^3 + 3R_p^2 h\right)$$

ω_0 = rotational speed of tool

R_s = shoulder radius

R_p = pin radius

h = height of the pin

•Solutions were generally of the order 10^4 W/mm^3

TEMPERATURE CONTINUED

- Subsequent simulations to determine welding temperature were run and input into FLUENT via user defined C code
- Method inherently ignores transient state including initial plunge and TS ramp up; creates an isothermal model
- The Visco Plastic model used to determine flow stress and viscosity (σ_e and μ respectively)
- Weld plate region: visco-plastic material

VISCO-PLASTIC MODEL

- Seidel, Ulysse, Colegrove et al. implemented VP model very successfully at relatively low w_p
  - RS: 500 rpm
  - TS: 120 mm min^{-1} (5.11 in min^{-1})

- High w_p implies:
  - Increase RS or
  - Decrease TS

- Geometries use VP model with 10-13 fold parametric increase accurately

VISCO-PLASTIC MODEL

- The VP model determines stress as,

$$\sigma_e = \frac{1}{\alpha}\sinh^{-1}\left[\left(\frac{Z}{A}\right)^{\frac{1}{n}}\right] \qquad Z = \dot{\varepsilon}\exp\left(\frac{Q}{RT}\right)$$

- Viscosity is approximated as, $\mu = \frac{\sigma_e}{3\dot{\varepsilon}}$

- The model is therefore a function of Temperature, T, and the effective strain-rate, $\dot{\varepsilon}$

Constants and Variables

Z = Zener-Hollomon parameter

R = Universal gas constant

T = absolute temperature (K)

$\dot{\varepsilon}$ = effective strain-rate

α, A, n, and Q = material constants

AXIAL FORCE SIMULATION

- Smooth pin model: a reference pressure was included to compensate for the lack of an anvil (open domain)
  - $P_{ref} = F_Z/A_p$
- Threaded pin model includes anvil:
  - no reference pressure is necessary (closed domain)

PROCEDURE

- Experimental sequence performed by holding the TS constant and increasing the RS incrementally until the weld matrix set was either complete or excessive surface defect occurred

- Samples etched for inspection for worm-holes (low w_p)

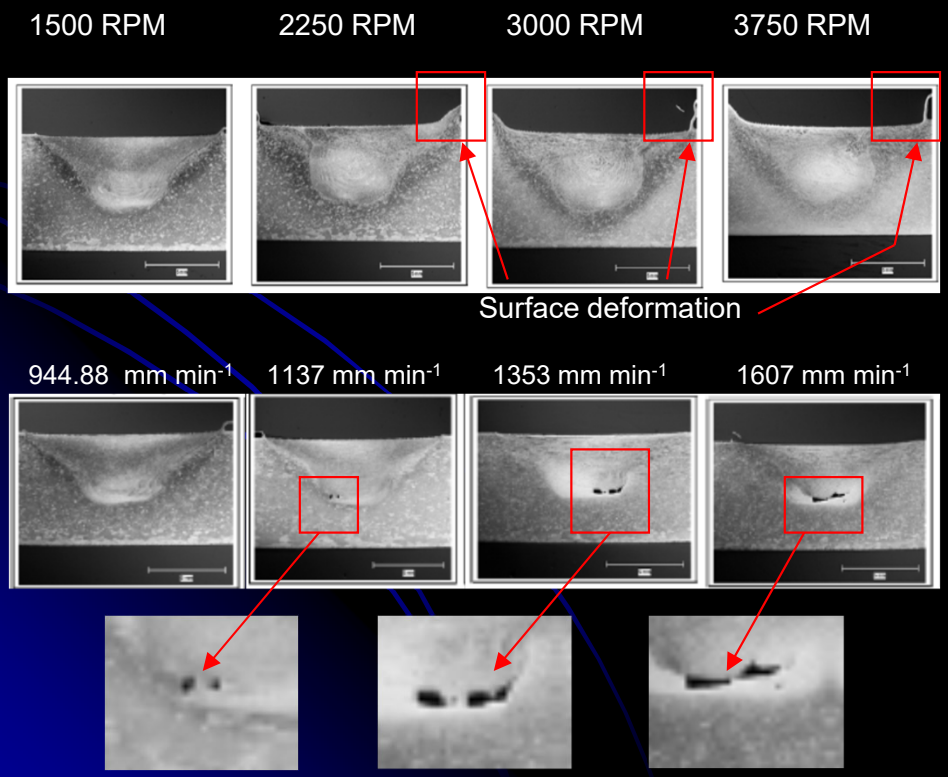

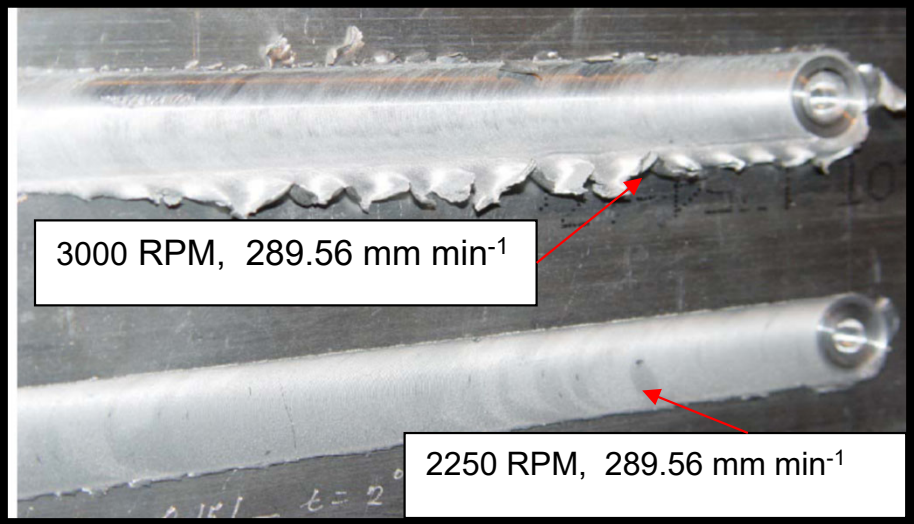

RESULTS

- Both models correlate well with experimental results
- Greater convergence at high w_p
- Increased RS/decreased F_z relationship continues for high speed FSW

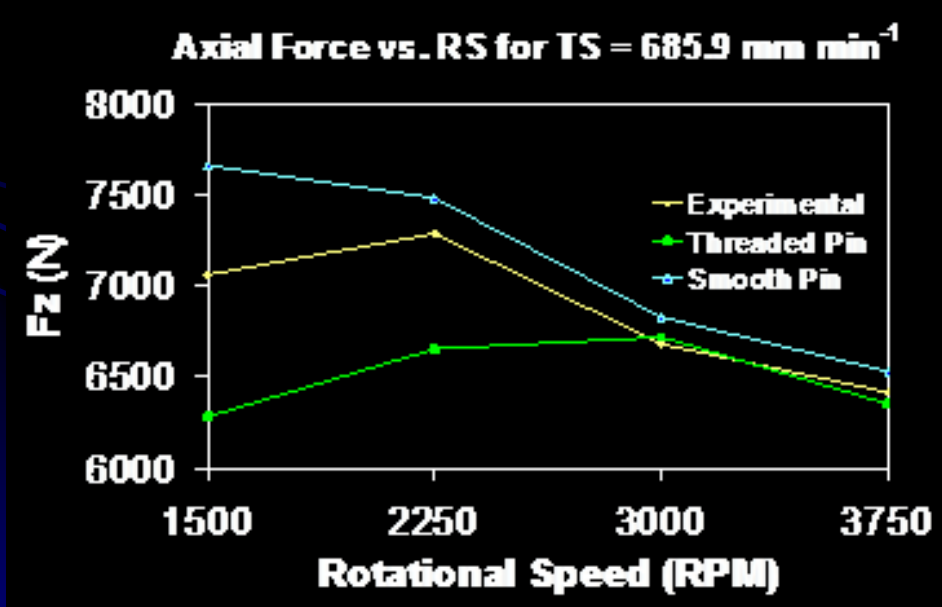

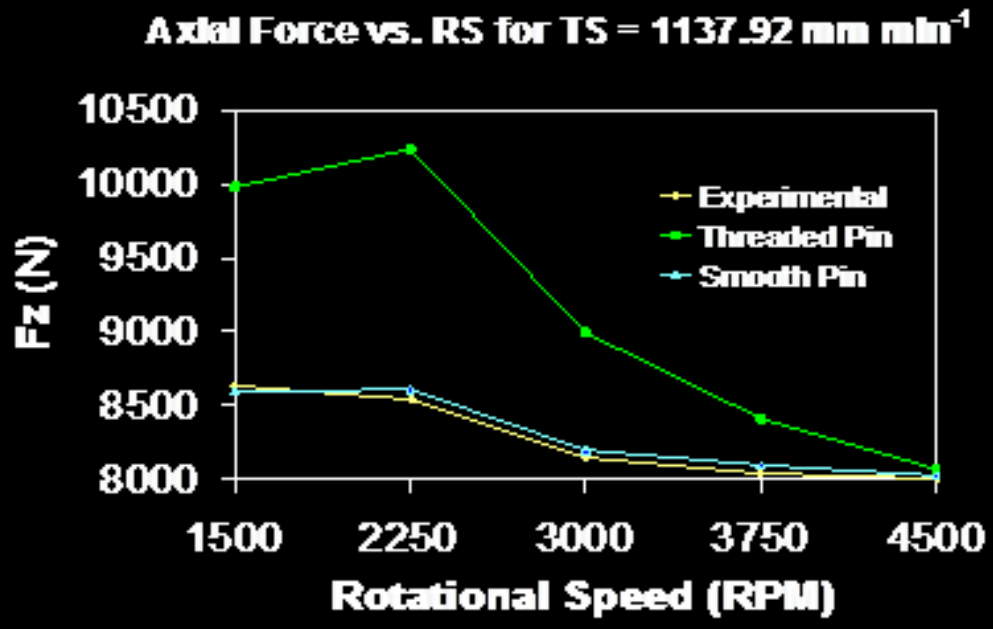

TS=685.9mm min^{-1} (27 in min^{-1})

TS=1137.92mm min-1 (44.8 in min-1)

RESULTS

- F_z increases as expected for increasing TS when RS constant
- Limit to the RS increase/F_z decrease not met
- This relationship is key to widespread implementation of FSW
- It is also well known that welding torque decreases for increased RS
  - M_z<50 N @ RS>1500 rpm (M_z<13 lbs)

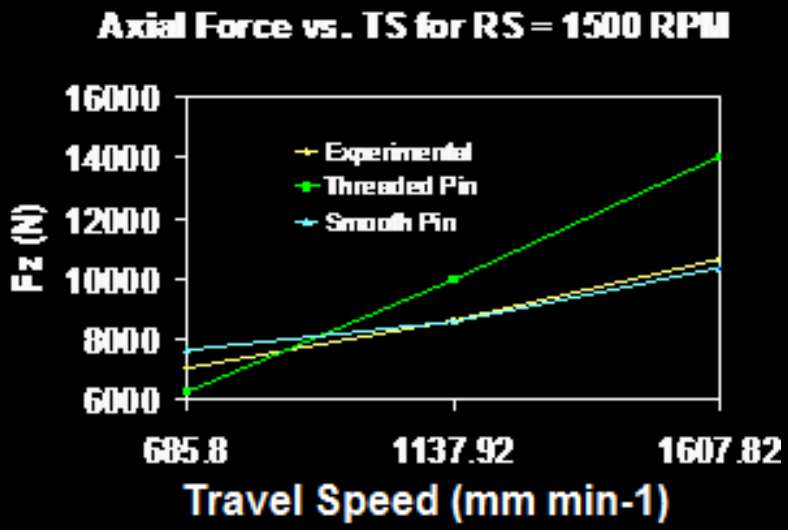

F_z vs. TS for RS = 1500 rpm

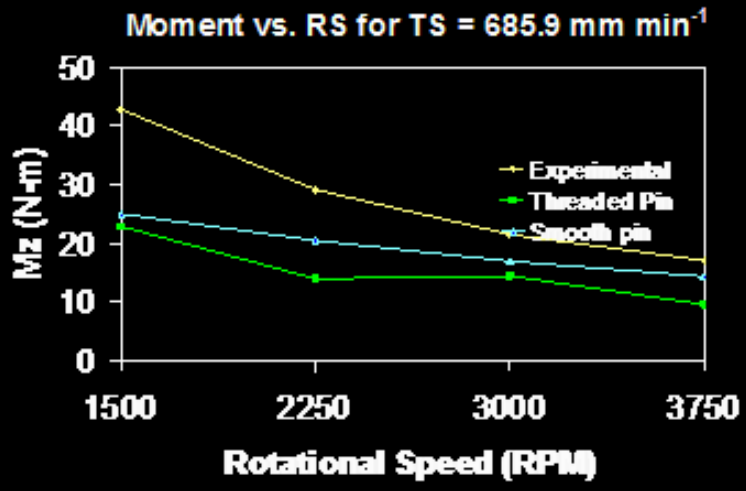

M_z vs. RS for TS = 685.9 mm min^{-1}

CONCLUSIONS

- The smooth pin model correlated better than the threaded pin model for all simulations
- However, threaded model more accurately represents the experimental setup
  - anvil, heat sinks, pin profile
- Increase in RS led to greater correlation in both models with respect to the experimental data
- Barrier to high speed FSW is overheating and subsequent surface flash

FUTURE WORK

- Possible solutions to high speed FSW problems
  - Non-rotating, floating, or differentially rotating shoulder
  - Implementing force control scheme
- Other control possibilities include acoustic signal analysis, temperature analysis, etc.
- Currently implementing three axes of linear position control as well as thermal imagery as a possible segway to future control schemes
- Latest rotational speeds exceeding 6500 RPM
- Latest travel speeds exceed 3810 mm min^{-1} (150 in min^{-1})
- Repeat using butt weld configuration and investigate unconventional weld defects through various stress testing

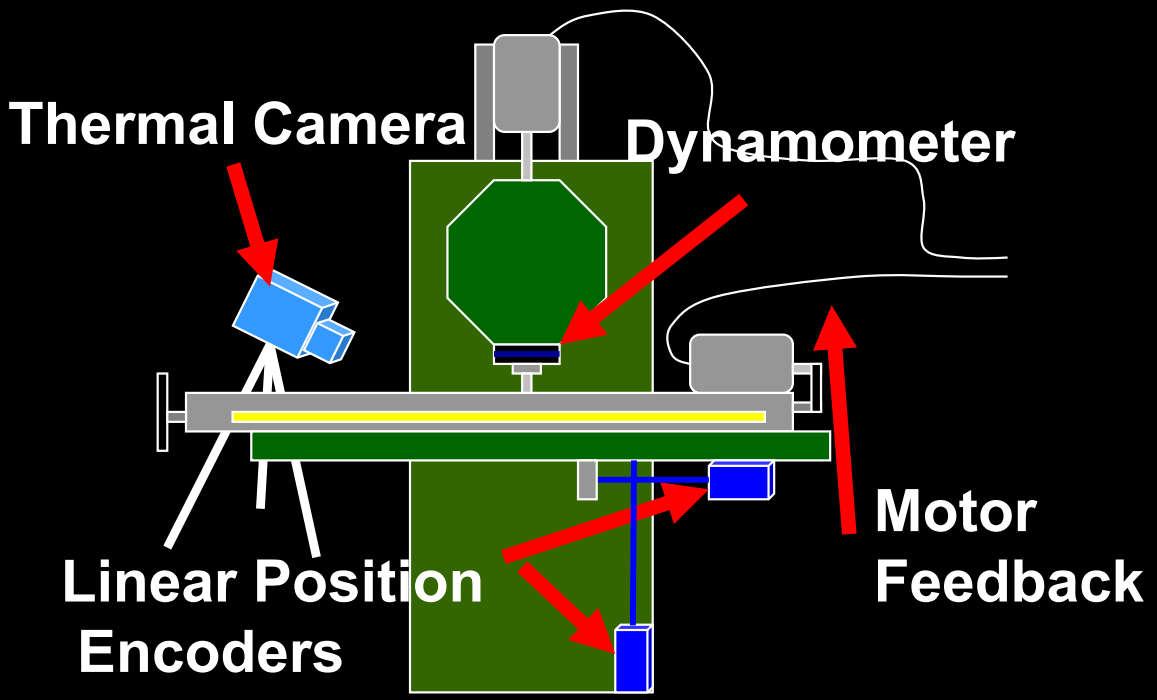

Schematic of most recent VUWAL data collection instrumentation

REFERENCES

- Cook G.E., Crawford R., Clark D.E. and Strauss A.M.: 'Robotic Friction Stir Welding'. Industrial Robot 2004 31 (1) 55-63.
- Mills K.C.: Recommended Values of Thermo-physical Properties for Commercial Alloys. Cambridge, UK 2002.
- Schmidt H., Hattel J. and Wert J.: 'An Analytical Model for the Heat Generation in Friction Stir Welding'. Modeling and Simulation in Materials Science and Engineering 2004 12 143–57.
- Crawford R: Parametric Quantification of Friction Stir Welding. M.S. Thesis, Vanderbilt University, Nashville, Tennessee 2005.
- Seidel T. U. and Reynolds A.P.: 'Two-dimensional friction stir welding process model based on fluid mechanics'. Science and Technology of Welding & Joining 2003 8 (3), 175-83.

REFERENCES

- Colgrove P.A. and Shercliff H.R.: ‘Development of Trivex friction stir welding tool Part 2 – three-dimensional flow modelling’. Science and Technology of Welding & Joining 2004, 9(3) 352-61.
- Ulysse P.: ’Three-dimensional modeling of the friction stir-welding process’ International Journal of Machine Tools & Manufacture 2002 42 1549–57.
- Sheppard T. and Jackson A.: ‘Constitutive equations for high flow stress of aluminum alloys’ Material Science and Technology 1997 13 203-9.
- FLUENT, Fluid Dynamic Analysis Package, version 6.122 Fluid Dynamics International, Evanston, IL.
- Talia G.E. and Chaudhuri J.: A Combined Experimental and Analytical modeling Approach to Understanding Friction Stir Welding. Department of Mechanical Engineering Presentation, Wichita State University, Wichita, KS 2004.